Matrix Padé approximants of the nucleon-nucleon interaction

A. Gersten and Z. Solow
Deparment of Physics, University of the Negev, Beer-Sheva, Israel
(Received 9 January 1974)

The matrix Padé approximants (with 16×16 matrices) and the scalar Padé approximants (with 4×4 matrices) of the nucleon-nucleon S-matrix elements are calculated for total angular momentum $J \leq 4$ and for laboratory kinetic energy up to 425 MeV. The calculations are based on one- and two-pion exchanges of the pseudoscalar interaction. The coupling constant g is the only parameter of the interaction for which a value, consistent with experimental results, $g^2/4\pi = 15$ is assumed. A simplified calculational scheme and formalism are presented. In order to interpret the results properly we give estimates in which energy regions we expect the one- and two-pion exchanges to be significant. For these energy regions we found that the matrix Padé approximants describe quite well the nucleon-nucleon interaction and give better approximations to the experimental data as compared to other methods of unitarization. The fact that in the framework of quantum field theory it is possible, even in limited energy regions, to give a reasonable description of the nucleon-nucleon scattering gives us more confidence in the pseudoscalar interaction as the fundamental interaction of nucleons and pions.

I. INTRODUCTION

In recent years a considerable amount of effort has been invested in calculating the amplitudes of the nucleon-nucleon (N-N) interaction.[1] The large number of experimental data and the reliable phase-shift analyses (up to 400 MeV lab energy) of the Yale[2] and Livermore[3] groups made possible a detailed comparison between theory and experiment.

The nucleon-nucleon interaction is peculiar, among other interactions, in that among the particles exchanged the pion has a mass much smaller than other exchanged particles. As a consequence, the partial waves with high angular momenta are dominated by the one-pion exchange (OPE). It is expected that for intermediate angular momenta the effect of the two-pion exchange (TPE) can be isolated and in this way more information about the form of the interaction can be supplied. The most favorite seems to be the interaction described by the interaction Lagrangian

$$L_{\text{Int}} = i g \bar{\psi} \gamma_5 \vec{\tau} \psi \vec{\phi} \ , \tag{1.1}$$

where ψ is the nucleon field, $\vec{\phi}$ is the charged pion field, and g is the coupling constant. In dealing with this interaction one encounters several difficulties. It is impossible at present to calculate the dressed propagators and vertices of the nucleons and pions. Only amplitudes corresponding to the skeleton TPE diagrams can be calculated. Thus many diagrams having the range of the TPE cannot be included in theoretical calculations. One way of overcoming this difficulty was initiated by Amati, Leader, and Vitale[4] (ALV) and by Goldberger, Grisaru, MacDowell, and Wong[5] (GGDW), who through dispersion theory correlate the pion-nucleon, pion-pion, and nucleon-nucleon scattering. The results obtained by using this approach are very encouraging,[6-9] but are based on additional phenomenological assumptions and thus cannot serve as a test of the fundamental interaction.

A direct test of a fundamental interaction is only possible for intermediate and higher partial waves. This can be done by calculating Feynman diagrams[10] or by solving the Bethe-Salpeter equation.[11] Here again many difficulties are encountered. The Bethe-Salpeter equation for the N-N interaction was solved only for the $^1S_0$ and $^3P_0$ states in the ladder approximation.[11] This work confirmed the predictions of Mandelstam[12] that for the ladder approximation and for low partial waves, there are no solutions for the pion-nucleon coupling constant having a value close to the experimental one ($g^2/4\pi \simeq 15$). For higher partial waves the convergence properties improve with the increase of the angular momentum.

The works of Gammel *et al.*[11,13] have demonstrated the usefulness of the Padé approximants. They have shown that accurate results can be obtained and that the convergence rate is superior to the perturbation expansion. The use of Padé approximants has many other advantages,[14,15] among which we should mention that unitarity is satisfied, and that bound states and resonances can be obtained (in contrary to the usual perturbation theory). Thus the Padé approximants seems to be a powerful tool for extracting information out of the perturbation expansion and, in this way, of testing the form of the fundamental interaction.

Gammel *et al.*[13] have shown, for the case of the Bethe-Salpeter equation, that the use of the so-

called matrix Padé approximants has an advantage over the usual Padé approximants, called S-matrix Padé approximants (SPA). Calculations with SPA have been done by Wortman[16] and by Bessis *et al.*[17]; most recent calculations with the [1/1] matrix Padé approximants have been done by Bessis, Turchetti, and Wortman[18] for total angular momentum $J \leq 4$ and by Fleischer, Gammel, and Menzel[19] for the $^1S_0$ and $^3P_0$ states. The formalism of Refs. 18 and 19 is somewhat different from ours (see Sec. IV), and therefore there is some difference between our results. Our intermediate steps are also done differently. In this respect our work is complementary to Refs. 18 and 19. The calculated $^1S_0$ and $^3P_0$ phase shifts differ in Refs. 18 and 19. The behavior of our results is similar to those of Ref. 19.

In our work we use the interaction Lagrangian (1.1). Our considerations are based on the Bethe-Salpeter equation. They are presented in Sec. II. The next sections deal with the formulas needed for computations, with presentation of the results and their evaluation.

Throughout our work we use the four-vector notation

$$x \equiv (x_1, x_2, x_3, x_4) \equiv (\vec{x}, x_4) \equiv (\vec{x}, i x_0) ,$$

and we use the Dirac γ matrices in the Dirac representation in which they are Hermitian. The spinors are normalized according to $\bar{u}_r u_s = \bar{v}_r v_s = \delta_{rs}$.

II. THE BETHE-SALPETER EQUATION

The scattering process is depicted in Fig. 1, where p_1 and p_2 are the four-momenta of the incoming nucleons, having spin projections in the direction of motion λ_1 and λ_2, respectively. The four-momenta of the outgoing nucleons are p_3 and p_4, with spin projections in the direction of motion λ_3 and λ_4, respectively. In the c.m. system

$$p_1 = (\vec{k}, ip_{10}), \quad p_2 = (-\vec{k}, ip_{20}),$$
$$p_3 = (\vec{q}, ip_{30}), \quad p_4 = (-\vec{q}, ip_{40}) .$$

The Mandelstam variables $s = -(p_1+p_2)^2$, $t = -(p_1-p_3)^2$ and $k = \frac{1}{2}(p_1-p_2)$, $q = \frac{1}{2}(p_3-p_4)$ will be used.

We employ the following form of the Bethe-Salpeter equation[20,21] for the M matrix (which is the T matrix stripped out of the spinors of the incoming and outgoing nucleons):

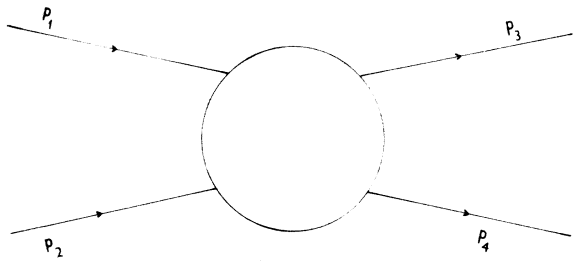

FIG. 1. The scattering of the two nucleons. The four-momenta of the incoming nucleons are p_1 and p_2, while p_3 and p_4 are the four-momenta of the outgoing nucleons.

$$M(p, q; s) = V(p, q; s) + \int d^4k\, V(p, k; s) G(k, s) M(k, q; s) . \tag{2.1}$$

V is composed from all irreducible Feynman diagrams. The M matrix is a 16×16 matrix in the spin space. The above equation can be converted[20] into a system of coupled matrix-element equations if we sandwich it with the positive- or negative-energy spinors with the momenta of the incoming and outgoing nucleons.

We introduce the following notation for the spinors:

$$u_{\lambda\epsilon}(\vec{p}) = \begin{cases} u_\lambda(\vec{p}) & \text{for } \epsilon = 1 \text{ (positive-energy spinor)} , \\ v_\lambda(\vec{p}) & \text{for } \epsilon = -1 \text{ (negative-energy spinor)} . \end{cases} \tag{2.2}$$

The negative-energy spinors and conjugate spinors are related to the positive-energy spinors via

$$v_\lambda(\vec{p}) = -\gamma_5 u_\lambda(\vec{p}), \quad \bar{v}_\lambda(\vec{p}) = \bar{u}_\lambda(\vec{p})\gamma_5 . \tag{2.3}$$

Equations (2.2) and (2.3) can be combined into

$$u_{\lambda\epsilon}(\vec{p}) = [\tfrac{1}{2}(1+\epsilon) I - \tfrac{1}{2}(1-\epsilon)\gamma_5]\, u_\lambda(\vec{p}) ,$$
$$\bar{u}_{\lambda\epsilon}(\vec{p}) = \bar{u}_\lambda(\vec{p})[\tfrac{1}{2}(1+\epsilon) I + \tfrac{1}{2}(1-\epsilon)\gamma_5] , \tag{2.4}$$

where I is a unit matrix. Using these relations we can construct the following matrix elements:

$$\langle \lambda_3\lambda_4\epsilon_3\epsilon_4 p | M(s) | \lambda_1\lambda_2\epsilon_1\epsilon_2 q \rangle = \bar{u}_{\lambda_3\epsilon_3}(\vec{p})\bar{u}_{\lambda_4\epsilon_4}(-\vec{p}) M(p, q; s) u_{\lambda_1\epsilon_1}(\vec{q}) u_{\lambda_2\epsilon_2}(-\vec{q}) , \tag{2.5}$$

for which one can obtain[20] the coupled equations

$$\langle \lambda_3\lambda_4\epsilon_3\epsilon_4 p | M(s) | \lambda_1\lambda_2\epsilon_1\epsilon_2 q \rangle = \langle \lambda_3\lambda_4\epsilon_3\epsilon_4 p | V(s) | \lambda_1\lambda_2\epsilon_1\epsilon_2 q \rangle + \sum_{\mu_1\mu_2\rho_1\rho_2} \int d^4k \langle \lambda_3\lambda_4\epsilon_3\epsilon_4 p | V | \mu_1\mu_2\rho_1\rho_2 k \rangle g(ks\rho_1\rho_2) \langle \mu_1\mu_2\rho_1\rho_2 k | M(s) | \lambda_1\lambda_2\epsilon_1\epsilon_2 q \rangle . \tag{2.6}$$

If we use successive approximations, the iterated solution (on the mass shell) can be written in the following way:

$$\langle\lambda_3\lambda_4\epsilon_3\epsilon_4 p|M(s)|\lambda_1\lambda_2\epsilon_1\epsilon_2 q\rangle = \sum_{n=1}\alpha^n\langle\lambda_3\lambda_4\epsilon_3\epsilon_4 p|M_{2n}(s)|\lambda_1\lambda_2\epsilon_1\epsilon_2 q\rangle \ , \quad (2.7)$$

where M_{2n} are all contributions to the M matrix coming from Feynman diagrams of order $2n$, and

$$\alpha = g^2/4\pi \ ,$$

where g is the coupling constant. Neither the existence of the solution nor the radius of convergence of the series expansion is known. The case when the radius of convergence is limited by poles of the coupling constant can be treated successfully by the use of Padé approximants.[22] The use of the Padé approximants is usually limited to the partial-wave equations with a definite total angular momentum J. As was shown in the work of Gammel *et al.*,[11,13] identical numerical solutions for the Bethe-Salpeter equation can be obtained either by using the matrix-inversion method or by Padé approximants.

On the basis of Eqs. (2.4) and (2.5) we can employ the Jacob and Wick[23] expansion, using only positive-energy two-particle states,

$$\langle\lambda_3\lambda_4\epsilon_3\epsilon_4 k|M(s)|\lambda_1\lambda_2\epsilon_1\epsilon_2 q\rangle = \frac{1}{4\pi}\sum_{J=0}(2J+1)\langle\lambda_3\lambda_4\epsilon_3\epsilon_4|M^J(s)|\lambda_1\lambda_2\epsilon_1\epsilon_2\rangle \times D^J_{\lambda_i\lambda_f}(\phi,\theta,-\phi) \ , \quad (2.8)$$

where $\lambda_i = \lambda_1 - \lambda_2$, $\lambda_f = \lambda_3 - \lambda_4$, and θ and ϕ are the polar angles of the scattered particles. Similar expansions are obtained for the terms appearing on the right-hand side of Eq. (2.7), from which we obtain (we suppress the dependence on s)

$$\langle\lambda_3\lambda_4\epsilon_3\epsilon_4|M^J|\lambda_1\lambda_2\epsilon_1\epsilon_2\rangle = \sum_{n=1}\alpha^n\langle\lambda_3\lambda_4\epsilon_3\epsilon_4|M^J_{2n}|\lambda_1\lambda_2\epsilon_1\epsilon_2\rangle \ . \quad (2.9)$$

Thus, the solutions of the Bethe-Salpeter equation can be expressed as power-series expansions with 16×16 matrix coefficients. The truncated expansion can be replaced by a matrix Padé approximant.[13] Before doing this let us simplify the notation.

III. ENUMERATION OF STATES AND THE PADÉ APPROXIMANT

In our work we deal with $16\times 16 = 256$ matrix elements characterized by different helicities and signs of energies. The enumeration convention used in Ref. 5 for the five independent matrix elements with positive energies is not suitable in our case. Instead, we introduce a new system of enumeration for the matrix elements:

$$\langle\lambda_3\lambda_4\epsilon_3\epsilon_4|M^J|\lambda_1\lambda_2\epsilon_1\epsilon_2\rangle \equiv M^J_{ij} \ . \quad (3.1)$$

The rules of correspondence between the number j and the numbers $\lambda_1\lambda_2\epsilon_1\epsilon_2$ are as follows: We write down the number $j-1$ in the binary system,

$$j-1 = b_0 + b_1\times 2 + b_2\times 2^2 + b_3\times 2^3 \ ,$$

and use the following rules of correspondence:

$$b_0 = \begin{cases} 0, & \text{for } \lambda_1 = \frac{1}{2} \\ 1, & \text{for } \lambda_1 = -\frac{1}{2} \ ; \end{cases}$$

$$b_1 = \begin{cases} 0, & \text{for } \lambda_2 = \frac{1}{2} \\ 1, & \text{for } \lambda_2 = -\frac{1}{2} \ ; \end{cases}$$

$$b_2 = \begin{cases} 0, & \text{for } \epsilon_1 = 1 \\ 1, & \text{for } \epsilon_1 = -1 \ ; \end{cases}$$

$$b_3 = \begin{cases} 0, & \text{for } \epsilon_2 = 1 \\ 1, & \text{for } \epsilon_2 = -1 \ . \end{cases}$$

For instance, for the state $|-\frac{1}{2}\,\frac{1}{2}\,-1\,1\rangle$ we have $j=6$. The same rules hold for the state $\langle\lambda_3\lambda_4\epsilon_3\epsilon_4|$ and the number i in Eq. (1.1). The relation between our system and that of Ref. 5, for $\epsilon_1=\epsilon_2=\epsilon_3=\epsilon_4$, is

$$\begin{aligned} &M^J_1 = M^J_{11} = M^J_{44}, \quad M^J_2 = M^J_{14} = M^J_{41} \ , \\ &M^J_3 = M^J_{33} = M^J_{22} \ , \quad M^J_4 = M^J_{32} = M^J_{23} \ , \\ &M^J_5 = M^5_{13} = M^J_{42} = M^J_{12} = M^J_{43} = M^J_{31} = M^J_{24} = M^J_{21} = M^J_{34} \ . \end{aligned} \quad (3.2)$$

Equation (2.9) can be replaced by

$$M^J_{ij} = \sum_{n=1}\alpha^n(M^J_{2n})_{ij}, \quad i,j = 1,2,\ldots,16 \ . \quad (3.3)$$

If we denote by M^J and M^J_{2n} the 16×16 matrices, which have the elements M^J_{ij} and $(M^J_{2n})_{ij}$, respectively, then Eq. (3.3) can be replaced by

$$M^J = \sum_{n=1}\alpha^n M^J_{2n} \ . \quad (3.4)$$

The [1/1] matrix Padé approximant (MPA) is[13,18]

$$[1/1]_{M^J} = \alpha M^J_2(M^J_2 - \alpha M^J_4)^{-1}M^J_2 \ . \quad (3.5)$$

The evaluation of M^J_2 and M^J_4 is the subject of Secs. IV–VI. The submatrices of M^J and M^J_{2n}, with matrix elements corresponding to $\epsilon_1=\epsilon_2=\epsilon_3=\epsilon_4=1$ (or M^J_{ij}, with $i,j=1,2,3,4$), can be used to form an S-matrix Padé approximant (SPA) in the form identical to Eq. (3.5). This SPA was used in the LS representation in Refs. 16 and 17. Our calculations with the MPA and SPA are made in the helicity representation. The final result is transformed

into the LS representation. The results should be independent of the representation used.[18]

IV. SECOND- AND FOURTH-ORDER TERMS

The M_2 and M_4 terms appearing in the iterated solution of the M-matrix equation (2.1) were worked out in Refs. 4, 7, and 16. The contributing irreducible diagrams to $V(p, q; s)$, and also to $M(p, q; s)$, are given in Fig. 2(a), and the iterated reducible diagram contributing to $M(p, q; s)$ is given in Fig. 2(b). The M_2 and M_4 terms are expressed with the aid of the ALV invariants[4,7,16], P_1, P_2, P_3, P_4, P_5, which are 16×16 matrices built up from a direct product of γ matrices. In order to calculate the matrix elements of M_2 and M_4, we need the matrix elements of the invariants P_i, $i = 1, 2, 3, 4, 5$. This will be done in Sec. V. In Sec. VI the isospin factors will be included. The scalar functions multiplying the invariants P_i were worked out in Refs. 4, 7, and 16, and will not be repeated here.

In our formalism, which utilizes the Bethe-Salpeter equation with dressed propagators and vertices, there is no place for the diagrams which are given in Fig. 3(a) and which are used in Ref. 18. These diagrams have zero matrix elements for $\epsilon_1 = \epsilon_2 = \epsilon_3 = \epsilon_4 = 1$ and therefore have no contribution to the SPA. If these diagrams would belong to $V(p, q; s)$ of Eq. (2.1) then the diagrams of Fig. 3(b) will appear three times in the iterated perturbation expansion of Eq. (2.7). Therefore the diagrams of Fig. 3(a) do not belong to the irreducible diagrams from which $V(p, q; s)$ is composed[24] and are not generated by the Bethe-Salpeter equation with dressed propagators and vertices. On the other hand, the diagrams of Fig. 3(a) are used (with a factor of $\frac{1}{2}$) in the Bethe-Salpeter equation with free propagators which was successfully used in bound-state problems of quantum electrodynamics.

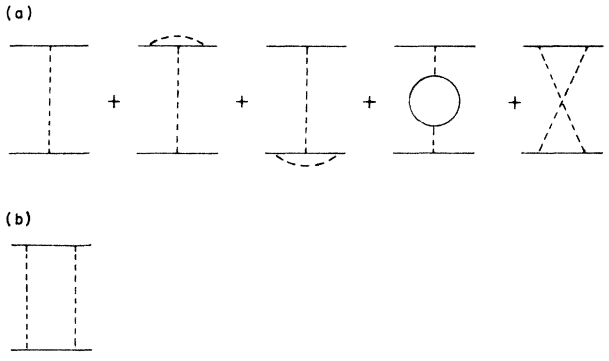

FIG. 2. Diagrams considered in our work. (a) The irreducible diagrams. (b) The reducible box diagram.

V. MATRIX ELEMENTS OF THE ALV INVARIANTS

The matrix elements of the P_i invariants can be calculated according to Eq. (2.5). We shall use the notation of Sec. II for the momenta p_1, p_2, p_3, p_4 of the incoming and outgoing particles. If

$$k = \tfrac{1}{2}(p_1 - p_2) = (\vec{k}, ik_0) ,$$

$$q = \tfrac{1}{2}(p_3 - p_4) = (\vec{q}, iq_0) ,$$

then on the mass shell

$$k_0 = q_0 = 0 .$$

We shall define

$$|\vec{k}| = |\vec{q}| = p ,$$

$$E = (p^2 + M^2)^{1/2} ,$$

$$W = M + E ,$$

where M is the nucleon mass. For a concise presentation of the lengthy results we shall introduce the notation

$$A_{ij} = (\epsilon_i + \epsilon_j)(W^2 - 4p^2\lambda_i\lambda_j) - 2pW(\epsilon_i - \epsilon_j)(\lambda_i - \lambda_j) ,$$

$$F_{ij} = (\epsilon_i - \epsilon_j)(W^2 - 4p^2\lambda_i\lambda_j) - 2pW(\epsilon_i + \epsilon_j)(\lambda_i - \lambda_j) ,$$

$$X_{ij} = (1 - \epsilon_i\epsilon_j)(W^2 + 4p^2\lambda_i\lambda_j) + 2pW(1 + \epsilon_i\epsilon_j)(\lambda_i + \lambda_j) ,$$

$$Y_{ij} = (1 + \epsilon_i\epsilon_j)(W^2 + 4p^2\lambda_i\lambda_j) + 2pW(1 - \epsilon_i\epsilon_j)(\lambda_i + \lambda_j) ,$$

$$N = 1/(4MW)^2 .$$

With these notations and Eqs. (2.5) and (2.4), we obtain after lengthy but straightforward calculations (with polar angle $\phi = 0$)

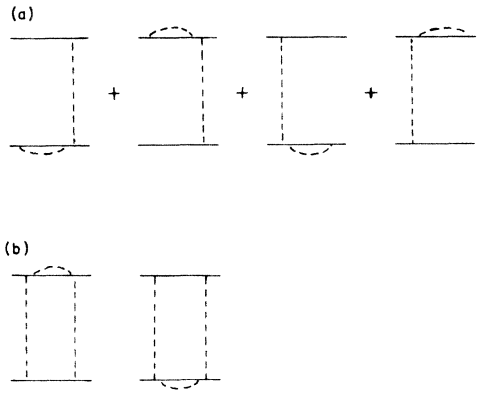

FIG. 3. Reducible diagrams. (a) Diagrams not included in our formalism. (b) The resulting sixth-order diagrams.

$$\langle\lambda_3\lambda_4\epsilon_3\epsilon_4 k|P_1|\lambda_1\lambda_2\epsilon_1\epsilon_2 q\rangle = [\bar{u}_{\lambda_3\epsilon_3}(\vec{k})u_{\lambda_1\epsilon_1}(\vec{q})][\bar{u}_{\lambda_4\epsilon_4}(-\vec{k})u_{\lambda_2\epsilon_2}(-\vec{q})]$$
$$= NA_{13}A_{24}B(\lambda_1,\lambda_2,\lambda_3,\lambda_4,\theta)\,,$$

where

$$B(\lambda_1,\lambda_2,\lambda_3,\lambda_4,\theta) = \chi^\dagger_{\lambda_3} e^{i\sigma_y\theta/2}\chi_{\lambda_1}\chi^\dagger_{-\lambda_4}e^{i\sigma_y\theta/2}\chi_{-\lambda_2}$$
$$= \tfrac{1}{2}(\tfrac{1}{2}+2\lambda_1\lambda_3)(\tfrac{1}{2}+2\lambda_2\lambda_4)(1+\cos\theta) - \tfrac{1}{2}(\lambda_3-\lambda_1)(\lambda_4-\lambda_2)(1-\cos\theta)$$
$$+\tfrac{1}{2}[(\lambda_3-\lambda_1)(\tfrac{1}{2}+2\lambda_2\lambda_4) - (\lambda_4-\lambda_2)(\tfrac{1}{2}+2\lambda_1\lambda_3)]\sin\theta\,,$$

where χ_λ and σ_y are Pauli spinors and matrices, respectively,

$$\langle\lambda_3\lambda_4\epsilon_3\epsilon_4 k|P_2|\lambda_1\lambda_2\epsilon_1\epsilon_2 q\rangle = \tfrac{1}{2}i[\bar{u}_{\lambda_3\epsilon_3}(\vec{k})\gamma\cdot(p_2+p_4)u_{\lambda_1\epsilon_1}(\vec{q})][\bar{u}_{\lambda_4\epsilon_4}(-\vec{k})u_{\lambda_2\epsilon_2}(-\vec{q})]$$
$$+\tfrac{1}{2}i[\bar{u}_{\lambda_3\epsilon_3}(\vec{k})u_{\lambda_1\epsilon_1}(\vec{q})][\bar{u}_{\lambda_4\epsilon_4}(-\vec{k})\gamma\cdot(p_1+p_3)u_{\lambda_2\epsilon_2}(-\vec{q})]$$
$$= -N\{A_{13}[p(\lambda_2+\lambda_4)X_{24}+EY_{24}]+[p(\lambda_1+\lambda_3)X_{13}+EY_{13}]A_{24}\}B(\lambda_1,\lambda_2,\lambda_3,\lambda_4,\theta)\,,$$

$$\langle\lambda_3\lambda_4\epsilon_3\epsilon_4 k|P_3|\lambda_1\lambda_2\epsilon_1\epsilon_2 q\rangle = -[\bar{u}_{\lambda_3\epsilon_3}(\vec{k})\gamma\cdot(p_2+p_4)u_{\lambda_1\epsilon_1}(\vec{q})][\bar{u}_{\lambda_4\epsilon_4}(-\vec{k})\gamma\cdot(p_1+p_3)u_{\lambda_2\epsilon_2}(-\vec{q})]$$
$$= N[p(\lambda_1+\lambda_3)X_{13}+EY_{13}][p(\lambda_2+\lambda_4)X_{24}+EY_{24}]B(\lambda_1,\lambda_2,\lambda_3,\lambda_4,\theta)\,,$$

$$\langle\lambda_3\lambda_4\epsilon_3\epsilon_4 k|P_4|\lambda_1\lambda_2\epsilon_1\epsilon_2 q\rangle = [\bar{u}_{\lambda_3\epsilon_3}(\vec{k})\gamma u_{\lambda_1\epsilon_1}(\vec{q})]\cdot[\bar{u}_{\lambda_4\epsilon_4}(-\vec{k})\gamma u_{\lambda_2\epsilon_2}(-\vec{q})]$$
$$= N[Y_{13}Y_{24}B(\lambda_1,\lambda_2,\lambda_3,\lambda_4,\theta)+X_{13}X_{24}C(\lambda_1,\lambda_2,\lambda_3,\lambda_4,\theta)]\,,$$

where

$$C(\lambda_1,\lambda_2,\lambda_3,\lambda_4,\theta) = \chi^\dagger_{\lambda_3}e^{i\sigma_y\theta/2}\vec{\sigma}\chi_{\lambda_1}\cdot\chi^\dagger_{-\lambda_4}e^{i\sigma_y\theta/2}\vec{\sigma}\chi_{-\lambda_2}$$
$$= \tfrac{1}{2}(\tfrac{1}{2}-2\lambda_1\lambda_2)(\tfrac{1}{2}-2\lambda_3\lambda_4) - \tfrac{3}{2}(\lambda_1+\lambda_2)(\lambda_3+\lambda_4)\tfrac{1}{2}[(\lambda_3-\lambda_1)(\lambda_4-\lambda_2)+(\tfrac{1}{2}+2\lambda_1\lambda_3)(\tfrac{1}{2}+2\lambda_2\lambda_4)]\cos\theta$$
$$+\tfrac{1}{2}[(\lambda_3-\lambda_1)(\tfrac{1}{2}+2\lambda_2\lambda_4) - (\lambda_4-\lambda_2)(\tfrac{1}{2}+2\lambda_1\lambda_3)]\sin\theta$$

and

$$\langle\lambda_3\lambda_4\epsilon_3\epsilon_4 k|P_5|\lambda_1\lambda_2\epsilon_1\epsilon_2 q\rangle = [\bar{u}_{\lambda_3\epsilon_3}(\vec{k})\gamma_5 u_{\lambda_1\epsilon_1}(\vec{q})][\bar{u}_{\lambda_4\epsilon_4}(-\vec{k})\gamma_5 u_{\lambda_2\epsilon_2}(-\vec{q})]$$
$$= NF_{13}F_{24}B(\lambda_1,\lambda_2,\lambda_3,\lambda_4,\theta)\,.$$

VI. ISOTOPIC-SPIN CONSIDERATIONS

The exchange of charged particles leads to the appearance of exchange diagrams. Equation (1.1) can be written as

$$L_{\rm int} = ig(\bar{p}p\pi^0 - \bar{n}n\pi^0 + \sqrt{2}\,\bar{n}p\pi^- + \sqrt{2}\,\bar{p}n\pi^+)\,, \tag{6.1}$$

where p and n are the proton and neutron fields, respectively, and π^+, π^0, π^- are the charged-pion fields. If the same mass is assumed for protons and neutrons and the same mass for charged and neutral pions, then the proton-neutron interaction, up to the fourth order in the coupling constant, is described by the sum of direct and exchange diagrams of Fig. 4.

Let us consider a contribution of a direct diagram M_D to the partial wave J (for the polar angle $\phi = 0$):

$$\langle\lambda_3\lambda_4\epsilon_3\epsilon_4|M^J_D|\lambda_1\lambda_2\epsilon_1\epsilon_2\rangle\, d^J_{\lambda_i\lambda_f}(\theta)\,, \tag{6.2}$$

with $\lambda_i = \lambda_1 - \lambda_2$ and $\lambda_f = \lambda_3 - \lambda_4$. The contribution of the corresponding exchange diagram $M_{\rm ex}$ is obtained by interchanging the particles 3 and 4. This leads to

(1) the interchange of all quantum numbers with indices 3 by the index 4 and vice versa,

(2) the replacement of θ by $\theta - \pi$ [from the relation

$$d^J_{\lambda_i,-\lambda_f}(\theta-\pi) = (-1)^{J-\lambda_f}d^J_{\lambda_i\lambda_f}(\theta)$$

we conclude that this has an effect of multiplying the amplitude by a factor $(-1)^{J-\lambda_f}$], and

(3) a change in the Jacob-Wick[23] phase factor of the two-particle states by $(-1)^{\lambda_f}$.

The final relation is

$$\langle\lambda_3\lambda_4\epsilon_3\epsilon_4|M^J_{\rm ex}|\lambda_1\lambda_2\epsilon_1\epsilon_2\rangle$$
$$= (-1)^J\langle\lambda_4\lambda_3\epsilon_4\epsilon_3|M^J_D|\lambda_1\lambda_2\epsilon_1\epsilon_2\rangle\,. \tag{6.3}$$

Thus we see that it is sufficient to calculate the contributions of direct diagrams. The isotopic spin factors are taken care of by using Fig. 4 and Eq. (6.3). The partial-wave projections of the amplitudes corresponding to direct diagrams are the subject of Sec. VII.

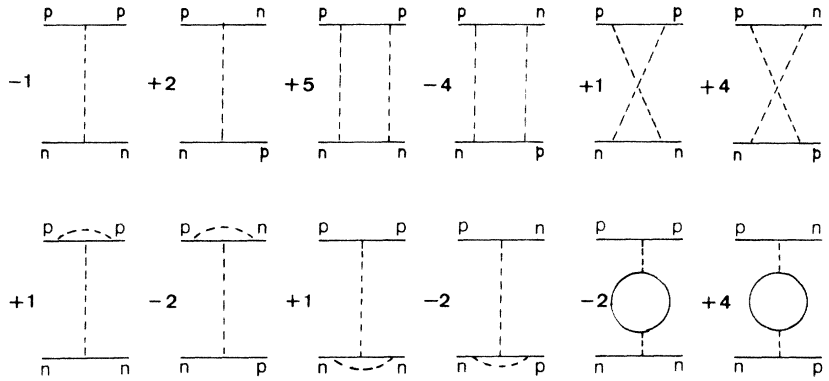

FIG. 4. The direct ($p+n \to p+n$) and exchange ($p+n \to n+p$) diagrams with proper factors.

VII. PARTIAL-WAVE PROJECTIONS

The contributions of the direct diagrams appearing in Fig. 4 can be presented in the following way:

$$M_D = \sum_{i=1}^{5} c_i(s,t) P_i , \tag{7.1}$$

where the P_i are the ALV invariants discussed in Sec. IV. The scalar coefficients $c_i(s,t)$ were derived elsewhere[4,7,16] and will not be repeated here. Their general form is

$$c_i(s,t) = \frac{1}{\pi}\int_{4\mu^2}^{\infty} \frac{\rho_1(t',s)\,dt'}{t'-t} + \frac{1}{\pi}\int_{4\mu^2}^{\infty} \frac{\rho_2(t',s)\,dt'}{t'+t+s+4m^2} . \tag{7.2}$$

The partial-wave projections in the form of Eq. (6.2) can be obtained if first the partial-wave expansions are made for

$$\frac{\langle \lambda_3\lambda_4\epsilon_3\epsilon_4 k|P_i|\lambda_1\lambda_2\epsilon_1\epsilon_2 q\rangle}{(t'-t)}, \quad i=1,2,3,4,5; \tag{7.3}$$

afterwards the integrals of Eq. (7.2) can be evaluated numerically. The procedure of deriving the partial-wave expansions of expressions like Eq. (7.3) or those of Sec. V was developed in other papers.[5,19,25,26,27] We shall present the final results only. On the basis of the results of Sec. V the expression of Eq. (7.3) has the following general form:

$$\langle \lambda_3\lambda_4\epsilon_3\epsilon_4 k|P_i|\lambda_1\lambda_2\epsilon_1\epsilon_3 q\rangle/(t'-t) = [\beta_i(\lambda_1,\lambda_2,\lambda_3,\lambda_4,\epsilon_1,\epsilon_2,\epsilon_3,\epsilon_4)B(\lambda_1,\lambda_2,\lambda_3,\lambda_4,\theta) + \gamma_i(\lambda_1,\lambda_2,\lambda_3,\lambda_4,\epsilon_1,\epsilon_2,\epsilon_3,\epsilon_4)C(\lambda_1,\lambda_2,\lambda_3,\lambda_4,\theta)]/(t'-t). \tag{7.4}$$

In the center-of-mass system

$$t = -2p^2(1-\cos\theta). \tag{7.5}$$

From Eqs. (7.4) and (7.5) we see that only the functions B, C, and $(t'-t)$ depend on θ, but not β_i nor γ_i. It is therefore sufficient to make the partial-wave expansions for

$$B(\lambda_1,\lambda_2,\lambda_3,\lambda_4,\theta)/(t'-t) = \frac{1}{4\pi}\sum_J (2J+1)B^J(\lambda_1,\lambda_2,\lambda_3,\lambda_4)\,d^J_{\lambda_i\lambda_f}(\theta), \tag{7.6}$$

with

$$\lambda_i = \lambda_1 - \lambda_2 \text{ and } \lambda_f = \lambda_3 - \lambda_4. \tag{7.7}$$

If we denote

$$x = 1 + t'/(2p^2), \quad \eta = \pi/p^2 \tag{7.8}$$

and use the convention of Sec. III in order to simplify the notation for $B^J(\lambda_1,\lambda_2,\lambda_3,\lambda_4)$ and $C^J(\lambda_1,\lambda_2,\lambda_3,\lambda_4)$, we obtain

$$\begin{aligned}
B^J_{11} &= \eta[(x+1)Q_J(x) - \delta_{J0}], \\
C^J_{11} &= \eta[(x-3)Q_J(x) - \delta_{J0}], \\
B^J_{14} &= \eta[(x-1)Q_J(x) - \delta_{J0}], \\
C^J_{14} &= \eta[(x+3)Q_J(x) - \delta_{J0}],
\end{aligned} \tag{7.9}$$

$$B^J_{33} = C^J_{33} = \eta\left[\frac{J}{2J+1}Q_{J+1}(x) + Q_J(x) + \frac{J+1}{2J+1}Q_{J-1}(x)\right],$$

$$B^J_{32} = C^J_{32} = \eta\left[\frac{J}{2J+1}Q_{J+1}(x) - Q_J(x) + \frac{J+1}{2J+1}Q_{J-1}(x)\right],$$

$$B^J_{13} = C^J_{13} = -\eta\frac{[J(J+1)]^{1/2}}{2J+1}[Q_{J+1}(x) - Q_{J-1}(x)],$$

where $Q_J(x)$ are the Legendre functions of the second kind. The remaining values of the B^J_{ij} and C^J_{ij} are obtained from Eq. (3.2).

With the aid of Eqs. (7.4) and (7.6)–(7.9) and by using the explicit values of the coefficients β_i and γ_i of Eq. (7.4) from Sec. V, the partial-wave expansions are directly obtained. These partial-wave expansions are given in the helicity representation. The transition to the LS representation is straightforward and is described elsewhere.[5,26,27]

VIII. UNITARITY AND THE IMAGINARY PART

In the M-matrix expansion given by Eq. (2.7) or by Eq. (3.4) it is sufficient to calculate the real parts of M^J_{2n}. The imaginary parts of M^J_{2n} can be obtained by using the generalized unitarity condition[18,20,27] for the Bethe-Salpeter equation

$$M^J - M^{J\dagger} = 2i\,\rho M^J \mathcal{P} M^{J\dagger}, \tag{8.1}$$

where $\mathcal{P}$ denotes that only positive-energy intermediate states are allowed, and ρ depends on the normalization convention. In the notation of Sec. III, Eq. (8.1) becomes

$$M^J_{ij} - M^{J\dagger}_{1j} = 2i\rho \sum_{n=1}^{4} M^J_{in} M^{J\dagger}_{nj}, \quad i,j = 1,\ldots,16. \tag{8.2}$$

In our calculations we used the normalization of Ref. 7 for which (using the notation of Sec. V)

$$\rho = M^2 p/(16\pi^2 E).$$

Equations (8.1) and (8.2) allow a simple way of computation of the imaginary parts of M^J_{2n} by inserting into them the expansions given by Eqs. (3.3) and (3.4). The required relations are obtained by comparing the terms appearing near the same powers of α. Thus we obtain, for energies above the elastic threshold,

$$\begin{aligned} &\mathrm{Im}(M^J_2) = 0, \\ &\mathrm{Im}(M^J_4) = \rho M^J_2 \mathcal{P} M^J_2, \\ &\mathrm{Im}(M^J_6) = \rho M^J_2 \mathcal{P}\,\mathrm{Re}(M^J_4) + \rho\,\mathrm{Re}(M^J_4)\mathcal{P} M^J_2, \quad \text{etc.} \end{aligned} \tag{8.3}$$

IX. RESULTS AND DISCUSSION

Before presenting our results it would be desirable to point out a few criteria which might be helpful in the final analysis. It is well known that the convergence of perturbation expansions is better for increasing values of the angular momentum L. Also range considerations are important. In a simplified way one can relate the impact parameter

$$b = [L(L+1)]^{1/2}/p \tag{9.1}$$

to the range of the multipion exchanges[28]

$$R = 1/n\mu, \tag{9.2}$$

where p is the c.m. momentum, μ the pion mass, and n the multiplicity of exchanged pions. The laboratory kinetic energy of the bombarding nucleons T_{lab} is related to p via

$$T_{\mathrm{lab}} = 2p^2/M, \tag{9.3}$$

where M is the nucleon mass. Equating Eqs. (9.1) and (9.2), we obtain that the characteristic kinetic energy corresponding to the n-pion exchange is

$$T_{nL} = \tau n^2 L(L+1), \tag{9.4}$$

where $\tau = 2\mu^2/M = 40$ MeV. We shall assume, following the ideas of Taketani,[29] that it is possible to separate the energy ranges below which the exchanges of more than n pions can be neglected. We shall assume that this can be done, similarly to Eq. (9.4), for energies

$$T_{\mathrm{lab}} < \tau_0 n^2 L(L+1). \tag{9.5}$$

In order to make a reasonable choice of the energy τ_0, we have studied the OPE contributions of References 10 and 16 versus the experimental data. It seems that for

$$\tau_0 \simeq 8 \text{ MeV} \tag{9.6}$$

and $n = 1$ the condition (9.5) is more or less satisfied. Thus, if we accept the conditions (9.5) and (9.6), we would expect the OPE + TPE to be significant for T_{lab} below about 64 MeV for P waves, 200 MeV for D waves, 400 MeV for F waves, 640 MeV for G waves, and below about 960 MeV for H waves. We should not expect the OPE + TPE to be significant for S waves and the mixing angle ϵ_1. Unless the coupling between the states with the same J is very small, the $^3D_1$ amplitude should be decoupled from the $^3S_1$ amplitude, the $^3F_2$ amplitude should be decoupled above about 64 MeV from the $^3P_2$ amplitude, and the ϵ_2 should not be significant above that energy. The $^3G_3$ amplitude should be decoupled from the $^3D_3$ amplitude above about 200 MeV and the ϵ_3 should not be significant above that energy. In deriving relation (9.5) we did not take into account whether the interaction is repulsive or attractive. For attractive interactions, the range becomes shorter; in this case we would expect a smaller value of τ_0 (for example, for the $^3P_2$ and $^3P_0$ states). For repulsive interactions (negative phase shifts) the range increases and a bigger τ_0 should be expected. All these considerations should be taken into account before comparing the results with the experimental data.

Our results are presented in Fig. 5, where for comparison the phase shifts of the Livermore[3] and Yale[2] groups, up to $T_{\mathrm{lab}} = 425$ MeV, are given.

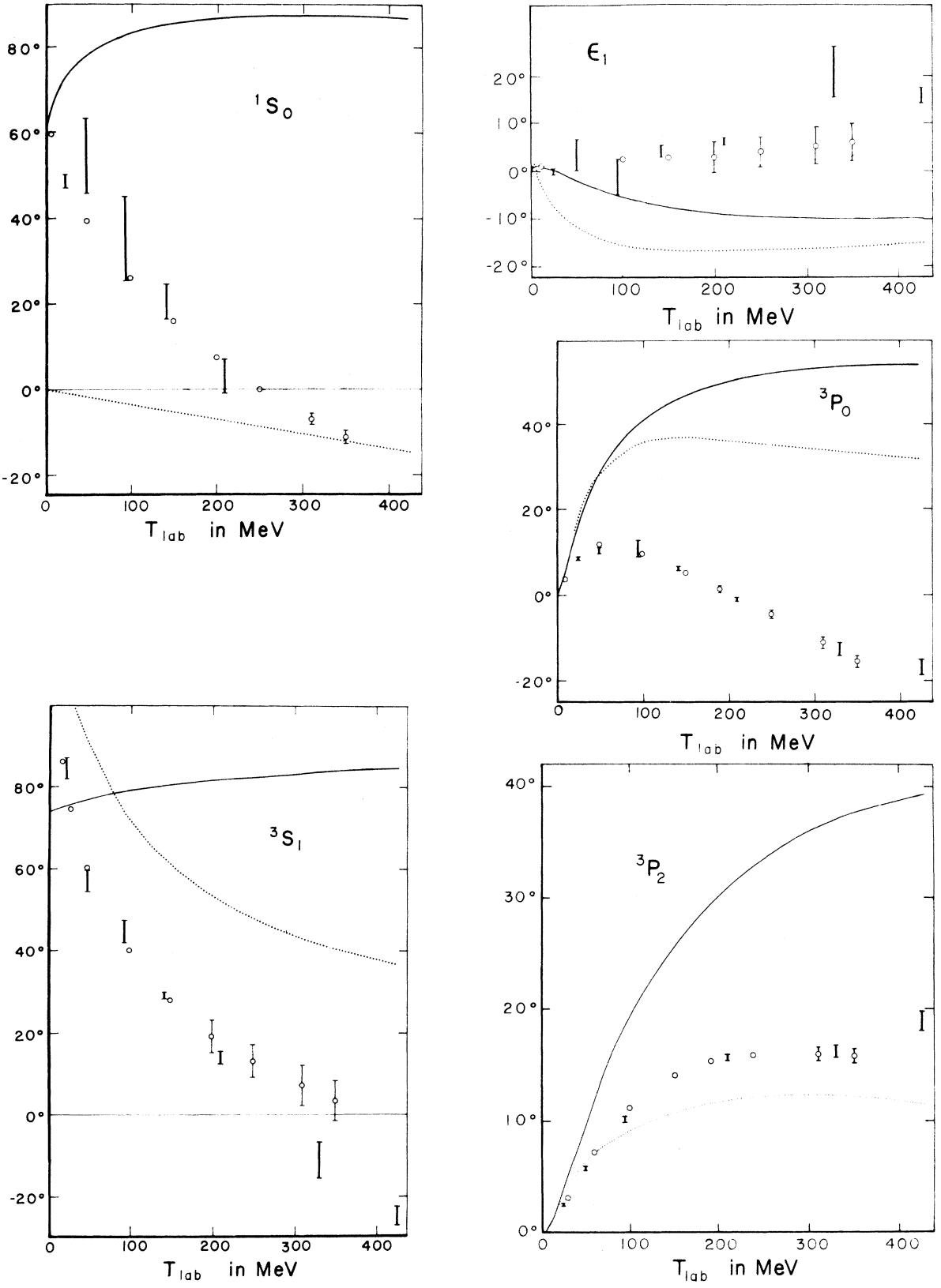

FIG. 5. *(Continued on following page.)*

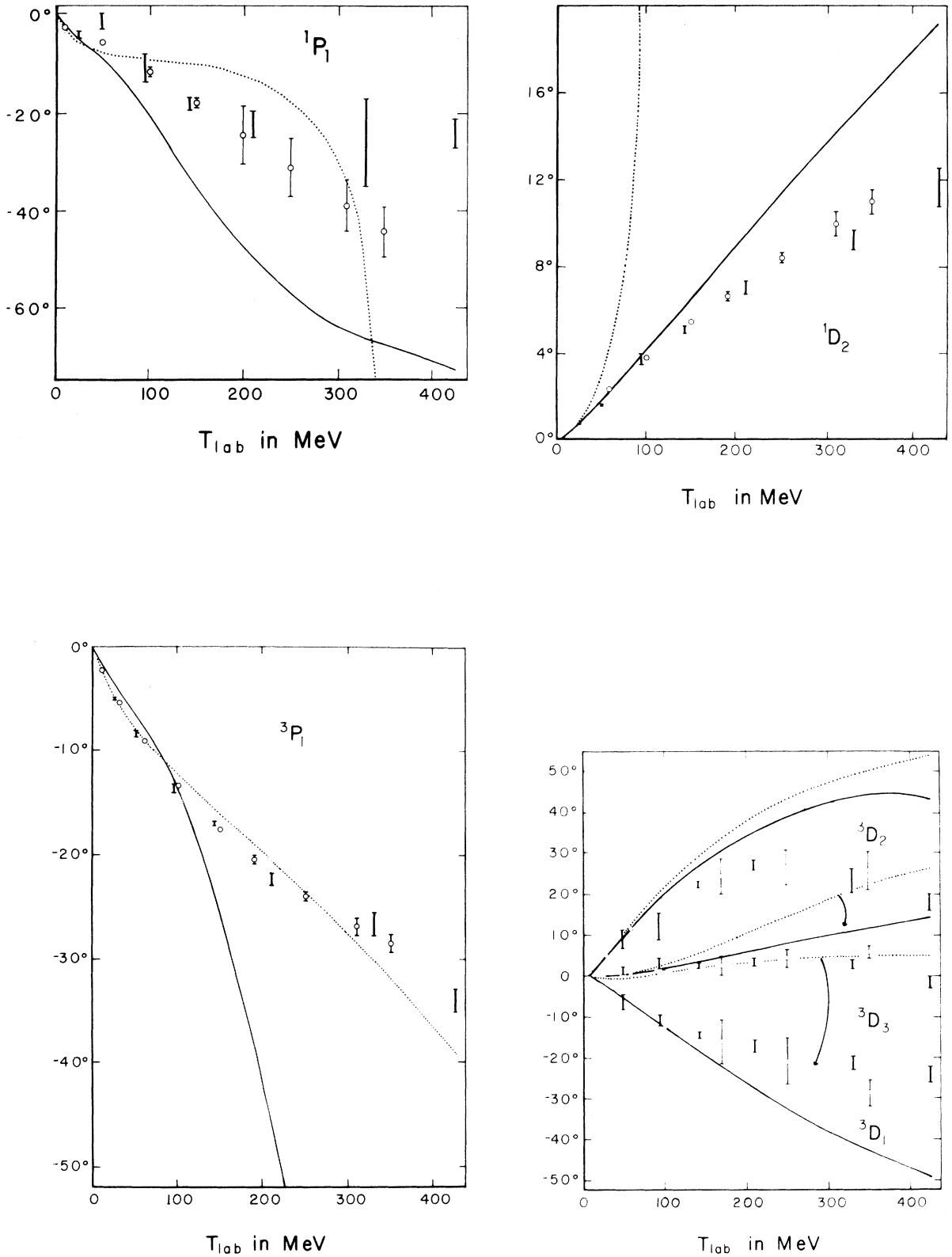

FIG. 5. *(Continued on following page.)*

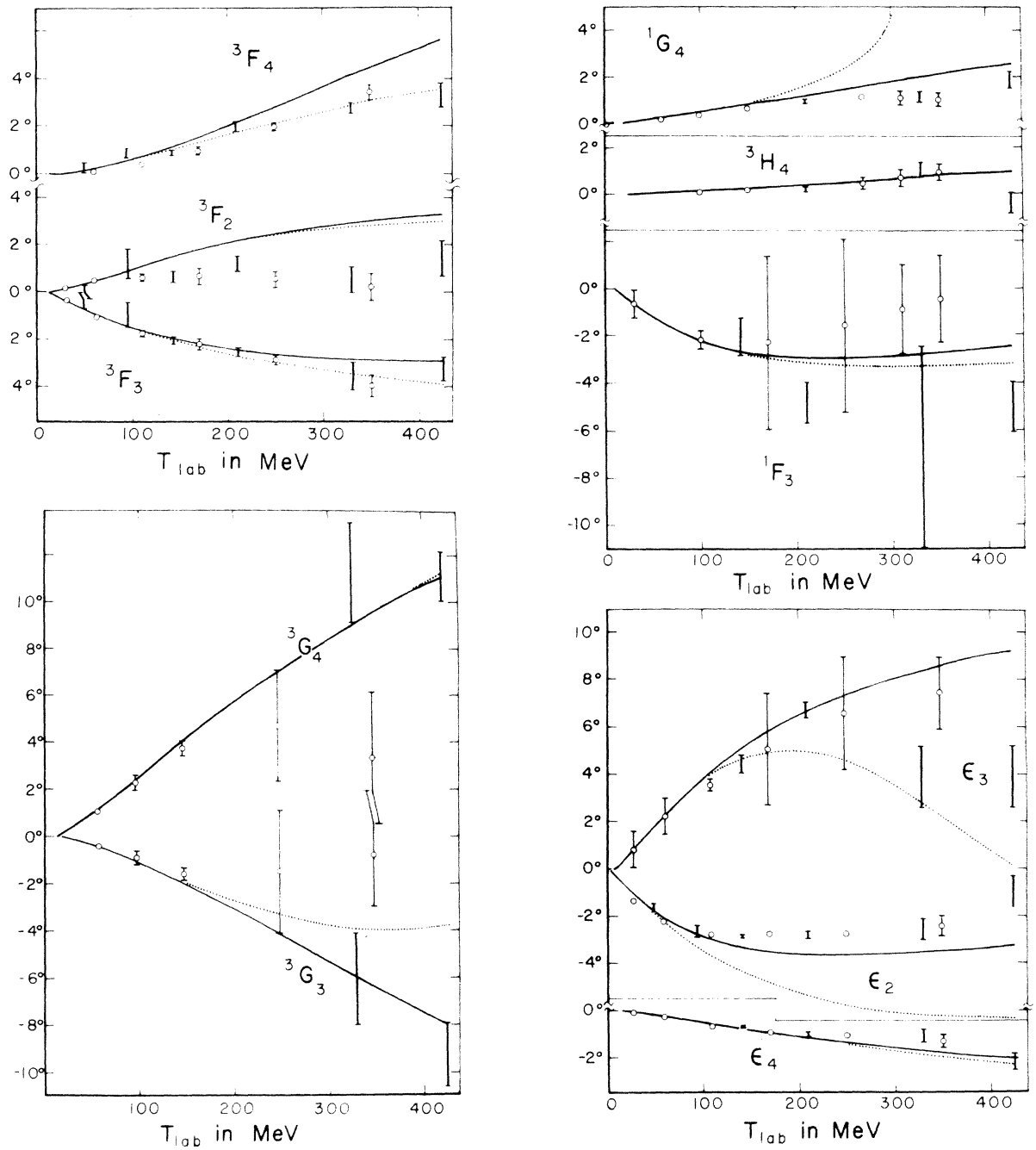

FIG. 5. Nucleon-nucleon nuclear-bar phase shifts calculated by using MPA's (solid line) and SPA's (dotted line). The heavy error lines depict experimental phase shifts found by the Livermore gorup (Ref. 3), while the circles and thin error lines correspond to an energy-dependent solution of the Yale group (Ref. 2). The phase shifts in degrees are given as a function of the laboratory kinetic energy T_{lab} in MeV.

Included are all phase shifts with $J \leq 4$. Our calculations were done with $\mu = 138$ MeV, $M = 938.5$ MeV, and $g^2/4\pi = 15$. Our results using the SPA agree completely with the results of Refs. 16 and 18. Our results using the MPA differ from the results of Ref. 18 for the reasons discussed in Sec. IV.

As it was already pointed out in Refs. 17 and 18, the SPA has some deficiencies, among which are the facts that the $^1D_2$ and $^1G_4$ pass through 90° and the $^1S_0$ has a bad threshold behavior. All these deficiencies are remedied by the use of the MPA.

Moreover, from the results presented, it appears that the MPA's for the energy ranges selected by us give a better approximation to the experimental data than the SPA. Our results should be compared with the results obtained by other methods of unitarization, namely with geometrical unitarization[16] (GU) and K-matrix unitarization[8,10] (KMU).

Below we summarize our findings:

Higher partial waves ($L \geq 3$). For the $^3H_4$, G, and F waves there is almost no difference between MPA's, GU, and KMU. The agreement with the experimental results is rather good, with some deviation in the $^3F_2$ phase shift which is coupled to the $^3P_2$ wave.

D waves below 200 MeV. We find a rather good agreement of the MPA with experimental phase shifts. The MPA shows an improvement for the $^3D_1$ phase shift over GU, KMU, and SPA.

P waves below 64 MeV. The MPA of the $^3P_1$ and $^1P_1$ is in agreement with experimental phase shifts. The $^3P_0$ and $^3P_2$ phase shifts (very similar to the GU and KMU phases) are larger than the experimental ones, but there is some quantitative agreement in their behavior. The discrepancy might be the result of a strong attraction, as discussed above.

Mixing angles. The ϵ_4, the ϵ_3 below 200 MeV, and the ϵ_2 below 64 MeV obtained by the MPA are in perfect agreement with experimental phase shifts. For the above energy ranges the MPA phases are similar to the GU and KMU ones. There is some improvement compared to the SPA. The bad agreement of the ϵ_1 should not be considered as a failure according to our previous considerations.

S waves. As we mentioned before, we should not expect the S-wave phase shifts to agree with the experimental data. However, it appears, at least for small energies, that there is some relation to the experimental phase shifts. With the SPA both S waves have a bound state: the $^3S_1$ with binding energy of 4.7 MeV and the $^1S_0$ with binding energy of about 5 MeV, 0.0004 MeV above the left-hand cut threshold of the OPE. The $^1S_0$ bound state is problematic since its appearance is caused by the singularity of the OPE at the left-hand cut threshold.[17] The $^3S_1$ and $^1S_0$ waves have no bound states with the MPA, but the phase shifts are quite large for small energies.

X. SUMMARY AND CONCLUSIONS

We started our considerations in Sec. II from the Bethe-Salpeter equation. We have shown how the iterated solution can be presented as a power-series expansion of the coupling constant. The expansion coefficients are 16×16 matrices. We were able to calculate the first two terms of that expansion due to previous work of Refs. 4, 7, and 16, where the M_2 and the M_4 terms were obtained using the Mandelstam representation. The explicit calculation of the matrix elements and their partial-wave expansion is done in Secs. III to VIII. The use of the helicity representation and our enumeration system of states of Sec. III greatly simplified the calculations. To this we may add Eq. (6.3) which in a simple way relates matrix elements of exchange diagrams to matrix elements of direct diagrams. This relation enabled us to include the isotopic spin factors while working in the helicity representation. The matrix Padé approximants were calculated in this representation; only the final results were converted to the LS representation. The nucleon-nucleon bar phase shifts were calculated and compared with experimental data up to 425 MeV laboratory kinetic energy.

The evaluation of the obtained results is a difficult task. The results are significant only if higher-order effects can be eliminated. We tried to attack this problem along the lines indicated by Taketani and coworkers[28,29] and to give estimates for energy regions where the one- and two-pion exchanges should dominate. This problem was discussed extensively in Sec. IX. The semiclassical concepts of impact-parameter relation to the range of the interaction were used. The energy regions were established by adopting the inequality (9.5) to the one-pion exchange. Thus, we obtained energy regions where the results are expected to be significant. Inside the limits of these regions we found that the phase shifts obtained with the [1, 1] matrix Padé approximants fit the experimental data relatively well. Moreover, they are in better agreement with the experimental data compared to other methods of unitarization. The use of the matrix Padé approximant corrected the failures of the S-matrix (or scalar) Padé approximants.

The fact that it is possible to explain the experimental data, even in restricted regions of energy, with a single theory, where the only parameter is the rather well-known coupling constant, give us more confidence in the existence of a fundamental interaction in the form of Eq. (1.1).

ACKNOWLEDGMENTS

One of us (A. G.) would like to thank Professor R. Vinh-Mau and Professor M. Lacombe for the kind hospitality extended to him at the Laboratoire

de Physique Théorique et Hautes Energies, University of Paris VI, during part of the summer, 1972. Fruitful discussions and information related to the two-pion exchanges obtained from them and Dr. J. M. Richard and Dr. B. Loiseau were essential in our work. The information given by Professor D. Bessis on the Padé approximants was very helpful to us.

[1]M. J. Moravcsik, Rep. Prog. Phys. 35, 587 (1972), and the large number of references quoted there.
[2]R. E. Seamon *et al.*, Phys. Rev. 165, 1579 (1968).
[3]M. H. MacGregor, R. A. Arndt, and R. M. Wright, Phys. Rev. 182, 1714 (1969).
[4]D. Amati, E. Leader, and B. Vitale, Nuovo Cimento 17, 68 (1960); 18, 409 (1960); 18, 458 (1960).
[5]M. L. Goldberger, M. T. Grisaru, S. W. MacDowell, and D. Y. Wong, Phys. Rev. 120, 2250 (1960).
[6]M. Chemtob, J. W. Durso, and D. O. Riska, Nucl. Phys. B38, 141 (1972).
[7]W. N. Cottingham *et al.*, Phys. Rev. D 8, 800 (1973).
[8]R. Vinh-Mau *et al.*, Univ. of Paris Report No. IPNO TH 73-04 (unpublished).
[9]J. Binstock and R. A. Bryan, Phys. Rev. D 4, 1341 (1971).
[10]B. M. Barker and R. D. Haracz, Phys. Rev. 186, 1624 (1969); J. L. Gammel and W. R. Wortman, J. Comput. Phys. 10, 568 (1972).
[11]J. L. Gammel, M. T. Menzel, and W. R. Wortman, Phys. Rev. D 3, 2175 (1971).
[12]S. Mandelstam, Proc. R. Soc. A237, 469 (1956).
[13]J. L. Gammel and M. T. Menzel, Phys. Rev. D 7, 565 (1973).
[14]*The Padé Approximant in Theoretical Physics*, edited by G. A. Baker and J. L. Gammel (Academic, New York, 1971).
[15]*Cargèse Lectures in Physics*, edited by D. Bessis (Gordon and Breach, New York, 1972), Vol. 5; *Padé Approximants*, edited by P. R. Graves-Morris (The Institute of Physics, London, 1973).
[16]W. R. Wortman, in Ref. 14.
[17]D. Bessis *et al.*, Phys. Rev. D 1, 2064 (1970).
[18]D. Bessis, G. Turchetti, and W. Wortman, Nuovo Cimento 22A, 157 (1974).
[19]J. Fleischer, J. L. Gammel, and M. T. Menzel, Phys. Rev. D 8, 1545 (1973).
[20]R. H. Thompson, Phys. Rev. D 1, 110 (1970).
[21]M. H. Partovi and E. L. Lomon, Phys. Rev. D 2, 1999 (1970).
[22]G. A. Baker, Jr., in *Advances in Theoretical Physics*, edited by K. A. Brueckner (Academic, New York, 1965), Vol. 1.
[23]M. Jacob and G. C. Wick, Ann. Phys. (N.Y.) 7, 404 (1959).
[24]S. S. Schweber, *An Introduction to Relativistic Quantum Field Theory* (Harper and Row, New York, 1961).
[25]A. Scotti and D. Wong, Phys. Rev. 138, B145 (1965).
[26]A. Gersten, R. H. Thompson, and A. E. S. Green, Phys. Rev. D 3, 2076 (1971).
[27]A. Gersten, P. A. Verhoeven, and J. J. de Swart, report (unpublished).
[28]M. Matsumoto and W. Watari, Prog. Theor. Phys. 11, 63 (1954).
[29]M. Taketani, S. Nakamura, and M. Sasaki, Prog. Theor. Phys. 6, 581 (1951).